ORIGINAL ARTICLE

In vitro evaluation of an iodine radionuclide dosimeter (IRD) for continuous patient monitoring

Sanaz Hariri Tabrizi [1] ⓘ · Meysam Ramezani [2] · Seyed Amir Hossein Feghhi [2] · Parham Geramifar [3]

Abstract

In vivo dosimetry of the patients treated by I-131 is important from patient dosimetry and radiation protection points of view. Knowledge of delivered dose to the target volume and adjacent normal tissues can improve the effectiveness of radioiodine treatment. Herein, design, fabrication, and assessment processes of an iodine radionuclide dosimeter (IRD) are explained. Two CsI(Tl) scintillator crystals coupled to photodiodes were used in IRD fabrication with specifications derived from Monte Carlo (MC) simulation. Linearity, sensitivity, and long-term performance of the system were tested. Delivered dose due to a known administered activity of I-131 was calculated by MC simulation which was validated based on the Medical Internal Radiation Dose (MIRD) Committee formalism, and the calibration factor was provided. Using the current mode signal acquisition method, the system showed a linear response up to 8.2 GBq radioiodine activity to prohibit the pile-up error without a need for correction factor. On the other hand, IRD was sensitive down to the rarely detectable activity of 7.4 MBq. A prototype version of the IRD system has been developed to guide the hospital staff for the safe release of iodine – administered patients and to provide an insight for physicians about the delivered dose to the thyroid and nearby organs.

Keywords Thyroid cancer · Radioiodine · Nuclear medicine · Dosimetry, patient monitoring

1 Introduction

Radioiodine therapy using I-131 is the standard treatment of thyroid remnant tissue after surgery and metastatic differentiated thyroid cancer. The prescribed activities for the first treatment to the metastatic disease range from 1.1 GBq to 9.3 GBq [1, 2]. Usually, the patients are treated with a fixed activity that is determined by the physician. It can result in overdosing and side effects such as lung fibrosis, bone marrow suppression, and sialadenitis or underdosing [1, 2]. However, administration of maximum allowable reasonably safe dose requires dosimetric approach for prescribing a patient-specific activity. It can be implemented by administration of a trace amount of I-131 to the patient and measuring the blood samples, whole body counting by a calibrated probe, and planar or tomographic gamma-camera imaging [1, 3]. Uptake measurement of I-123 or I-131 during a time period can result in the patient-specific effective half-life determination from which the total absorbed dose is estimated [4].

Another application for radioiodine dosimetry is from a safety point of view. There are several guidelines for the safe release of the iodine-treated patients from the hospital (e.g., ambient dose equivalent rate of less than 20 μSv/h at 1 m distance [4]). As there are several guidelines for the safe release of inpatients and outpatients treated with radioiodine, radiation exposure of the patient should be accurately measured to demonstrate that acceptance level has been reached [5]. Measurement of the patient dose can be accomplished using semiconductor-based electronic dosimeters [6], thermoluminescent dosimeters (TLD) [6], scintillator gamma probes [7], or Geiger–Müller (GM) detectors [8].

For all purposes of pre- and post-therapeutic patient dosimetry and public safety, the routine radiation detectors introduce some limitations. They include (1) invasive nature of blood sampling, (2) offline response of TLD, (3) subjective data collection by GM, (4) being time-consuming, (5) expensive and hazardous

✉ Sanaz Hariri Tabrizi
S_HaririTabrizi@sbu.ac.ir

1   Department of Medical Radiation Engineering, Shahid Beheshti University, G.C., Tehran, Iran

2   Radiation Application Department, Shahid Beheshti University, G.C., Tehran, Iran

3   Research Center for Nuclear Medicine, Shariati Hospital, Tehran University of Medical Sciences, Tehran, Iran

procedure of patient transportation to the imaging room due to staff overexposure, and (6) limited number of available data points for analysis applicable to all. Dynamic radioiodine uptake profile acquisition by a portable radiation detector system is more preferable than the routine pre-therapy I-123 uptake measurement using SPECT [4]. So far, measuring devices attachable to a cervical collar [9, 10] or neck strap [10] have been developed. The performance of a commercial measurement device called Collar Therapy Indication (CoTI) has been presented in [4, 9]. Because of the pulse mode signal acquisition method used in development of CoTI system, it suffers from nonlinear response in high activity radioiodine measurements. In this mode, each individual quantum of radiation interaction is recorded which can become impractical in high event rates. On the other hand, current mode radiation detector operation takes a time average of the deposited energy which is not affected by the exposure rate [11]. As another example of a portable dosimeter, reference [10] can be introduced, while the detailed specifications of the system have not been presented.

The purpose of this work is to develop and characterize a prototype version of a portable iodine radionuclide dosimeter (IRD). The performance of the device from linearity and susceptibility to long-term operation points of view is tested. Because of using current mode signal acquisition method, the system is expected to show a wide linear range of operation. Also, its reading is calibrated against analytically validated Monte Carlo (MC) simulation to show the absorbed dose in any organ of interest. Finally, the process of validating analytically calculated dose based on the Medical Internal Radiation Dose (MIRD) Committee formalism is explained.

2 Materials and methods

2.1 Iodine radionuclide dosimeter description

The developed thyroid monitoring system was composed of two CsI(Tl) scintillators coupled with two silicon photodiodes (type no. S1337-1010BR, Hamamatsu Co., Japan). Advantages of using CsI(Tl) crystal compared with NaI(Tl), which is applied in many diagnostic system constructions, include higher efficiency for the most frequent emitted gamma ray from I-131 (365 keV), higher efficiency when coupled with the mentioned photodiodes, less sensitivity to ambient condition [11], and less than 5% light yield variation for the energy range of I-131 gamma rays [12]. The optimum shape, dimension, and position of the crystals relative to the thyroid lobes were investigated using MC code MCNPX 2.6.0 [13]. In summary, it is a general purpose code for transporting the photon, electron, and many other particles in a medium introduced by its geometry and composition to the code. A neck phantom including two thyroid lobes and isthmus was simulated to examine if a single crystal covering both lobes

introduced a higher efficiency or separate cylindrical or cubic crystals with different diameters and lengths (ranging from 1 to 4 cm). Finally, it was found that two separate cubic crystals with the size of $30 \times 20 \times 5$ mm^3, besides having appropriate dimension for the clinical use, provided the highest efficiency among the tested ones. The simulations were run with 30 million histories which resulted in error values less than 0.3%.

The utilized photodiodes were smaller than the scintillator crystals and had a photosensitive size of 1×1 cm^2. Therefore, some silicone gel was applied between the crystals and photodiodes, and some Teflon tape and an aluminum reflector were used around the package. In addition, the system was put in a photo-resistant black box with coaxial cable output, to make the output (signal) detectable among the 50 Hz noise (Fig. 1). The radiation detector was setup in current mode to prevent probable pile-up errors in the high activity range, especially soon after I-131 administration. A current to voltage converter circuit as a preamplifier and an amplifier with a gain of 1000 was used for transforming the detected photons to voltage signal up to 15 V.

2.2 Phantom tests

2.2.1 Water mug

In order to test the system linearity, a water container with a similar thickness as human neck with a holder for a radioiodine vial in the middle was used. The two monitoring systems were attached to its outer surface (Fig. 2a).

2.2.2 MIHAN phantom

In order to calibrate the output voltage based on the delivered dose to the thyroid, to validate the estimated dose by MC method and to check the long-term performance of the system in a clinical equivalent condition, a multipurpose Iranian head and neck (MIHAN) phantom was used [14]. MIHAN phantom contains several inhomogeneities as a human being. The hollow thyroid of the phantom was filled with 0.4 GBq (9.8 mCi) I-131, and output voltages were recorded during
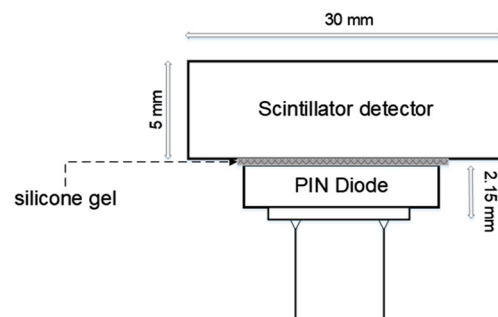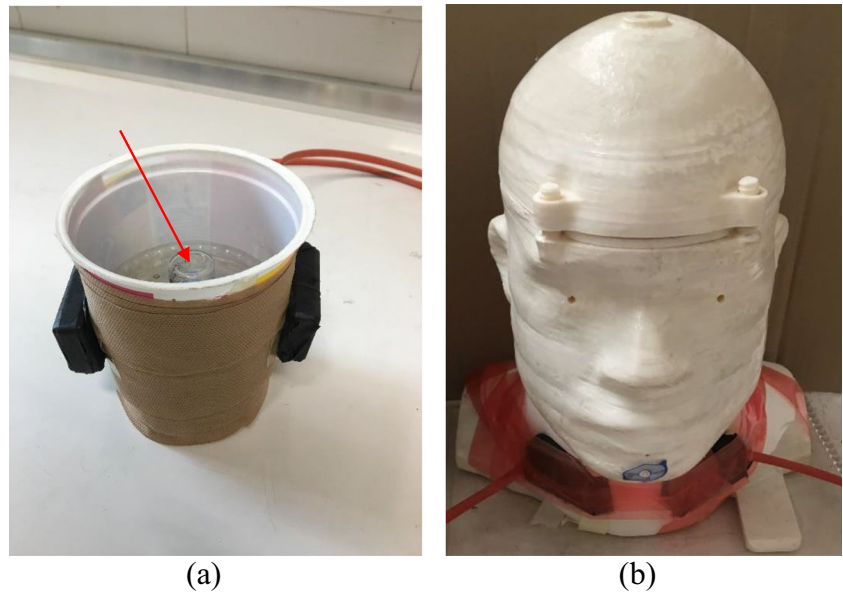

Fig. 1 A Schematic of constituents of the iodine radionuclide dosimeter system

Fig. 2 (a) A photograph of the water mug experiment with radioiodine vial in the middle (the red arrow), (b) the MIHAN phantom with the attached system. A marker for CT scan setup is seen on its chin

(a)   (b)

45 days after radioiodine administration (Fig. 2b). The precision of measurements was increased by averaging at least three measurements during every 3 min film recording from the IRD system reading.

2.3 Simulation validation

In order to estimate the absorbed doses in different organs and relate them to the system reading, MC simulation was performed. The results were validated by analytical calculation based on MIRD committee formalism. Each lobe of the thyroid can be assumed as an ellipsoidal volume of soft tissue with uniform distribution of activity. The absorbed fractions for the I-131-emitted gamma radiations were calculated based on the "generalized radius" concept introduced by Amato et al. [15]. They proposed a nonlinear relationship between the absorbed fraction, ϕ, and the generalized radius, ρ, as shown in eq. (1)

$$\phi(\rho) = \left(1 + \frac{\rho_0}{\rho^s}\right)^{-1} \tag{1}$$

in which ρ_0 and s are energy-dependent parameters fitted using Levenberg–Marquardt algorithm, and their values can be found elsewhere [15]. The absorbed fraction of the beta particles was assumed to be unit [16].

The MIHAN phantom was tomographic scanned, and different organs including thyroid were imported to the MCNP code (Fig. 3). The selected settings for CT image acquisition included 110 kVp, 170 mA, 0.5 mm resolution, and 2.4 mm slice thickness using a standalone SOMATOM Emotion Siemens CT scanner. Each lobe was encircled by a prolate ellipsoid, and the generalized radius was calculated according to [15]. Amato et al. have presented energy deposition per disintegration (ED) versus generalized radius of ellipsoidal volumes [15]. Accordingly, the

corresponding ED (keV/t) for uniform I-131 distribution was found. Comparison between the analytical (ED_{anal}) and simulated (ED_{sim}) energy deposition per disintegration was made after application of some correction factors.

The analytical calculation results in absorbed dose in an ellipsoid of soft tissue with uniform distribution of activity without any material surrounding it (i.e., in vacuo). However, absorbed dose in one phantom thyroid lobe was not only due to its own activity but also the other lobe and isthmus. In addition, the phantom was filled with water which produced back scattering of the emitted particles. In addition, deviation in the calculation and simulation results can be
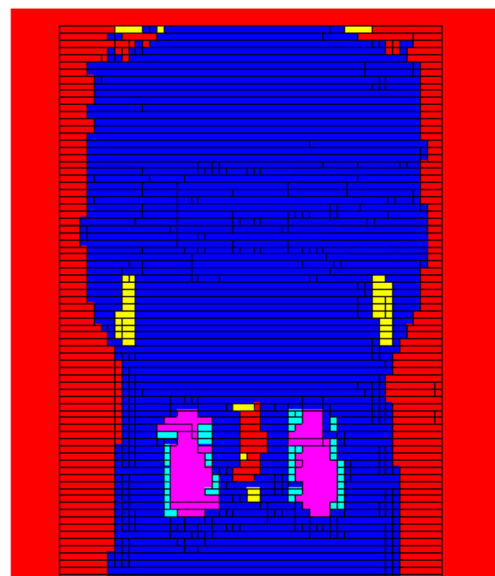

Fig. 3 Coronal view of the imported phantom to the MCNP code. The yellow parts show the mandible bone. Thyroid lobes are in pink, and the air in the trachea and the surrounding can be seen in red

attributed to some other factors including (1) differences between employed beta and gamma spectra of I-131 [16] and what was used by [15] and (2) the encircled ellipsoid and real thyroid cells in the MCNP code. In order to account for these differences, two additional situations were simulated: (1) one lobe (e.g., right) of the thyroid containing the mass-normalized I-131 activity in vacuo and (2) both lobes and isthmus in water environment with uniform distribution of whole activity and recording the absorbed dose in one of the lobes (e.g., right). Difference between the absorbed dose in the two simulations which accounts for the backscattering from surrounding material and activity in the other thyroid lobe was named as CF_1. Because the beta and gamma spectra used by [15] were different from the simulated ones [16], i.e., no x-rays and internal conversion electron or Auger electron was taken into account, another correction factor (CF_2) was used. It incorporated not only the spectra difference but also the shape difference with an ideal ellipsoid and was calculated as difference between simulation #1 and the MIRD-based ED. Application of the two correction factors resulted in the first modified ED in the right lobe based on the surrounding material and activity (ED'_{sim}) and the second modified ED that accounted for different emission spectra (ED''_{sim}) as follows:

$$ED'_{sim} = ED_{sim} - ED_{sim} \times CF_1 \qquad (2)$$

$$ED''_{sim} = ED'_{sim} + ED'_{sim} \times CF_2 \qquad (3)$$

Combination of the two equations resulted in the percent dose difference (%DD) as follows:

$$\%DD = 100 \times \frac{ED_{anal} - ED_{sim}(1 - CF_1)(1 + CF_2)}{ED_{anal}} \qquad (4)$$

It is worth noting that energy deposition per particle in MeV/t was recorded in all MCNP simulations. The number of transported gamma and beta particles was between 6 hundred thousand and 2 million to achieve less than 1% variation in the results.

3 Results

3.1 System linearity

Four calibrated radioiodine vials containing 8.5, 40.6, 103.0, and 221.0 mCi activities were positioned in the water mug, and the voltage output from the two monitoring systems was recorded (Fig. 4a). Linear response of both systems without saturation, even for an extreme value of 221.0 mCi, is obvious. For far less activities with less safety hazards, the linearity of the system number 1 was checked in MIHAN phantom, too (Fig. 4b).
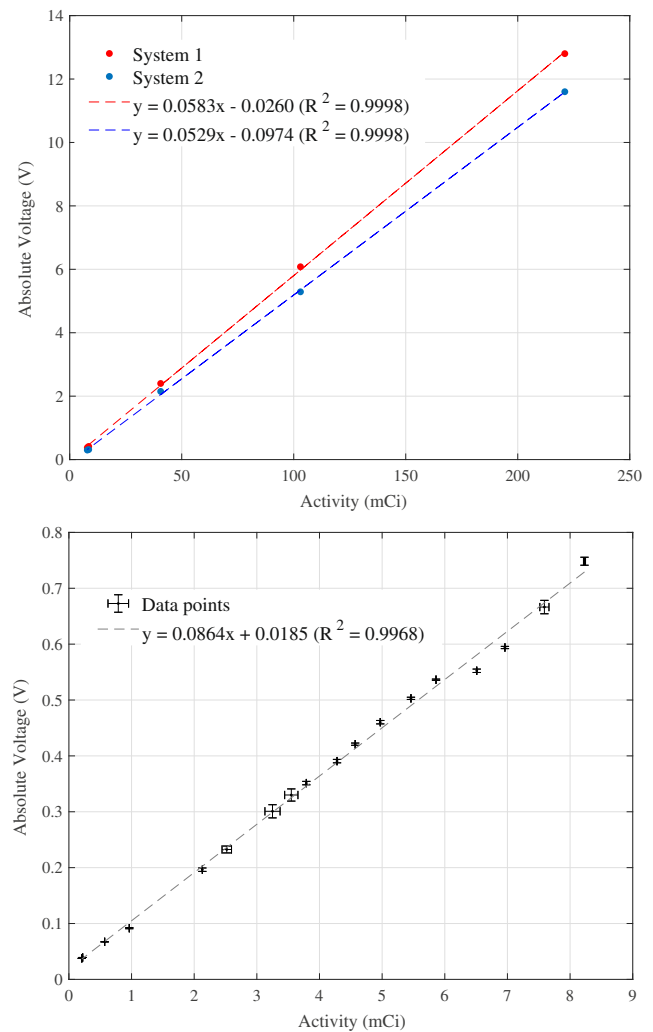

Fig. 4 Linearity test in the (a) water mug and (b) MIHAN phantom. Systems 1 and 2 indicate the two dosimeters positioned opposite each other around the mug. Error bars show the 95% confidence interval of measurements (k = 2)

3.2 Long-term performance

During 45 days after filling the thyroid of MIHAN phantom with 0.4 GBq (9.8 mCi) of I-131, 18 measurements were done for system 1. The measurements were done to provide the data points in Fig. 4b and to compare the obtained decay constant with the expectation (Fig. 5).

3.3 System calibration

The generalized radius (ρ) for the right and left lobes was found to be 1.0 cm and 1.1 cm, respectively. Based on [15], they corresponded to I-131 ED of about 197 and 199 keV/t, respectively. While the mean value for analytical calculation corresponded to 198 keV/t, the obtained ED from simulation number 1 introduced in section 2.3 was 184 keV/t. It was in
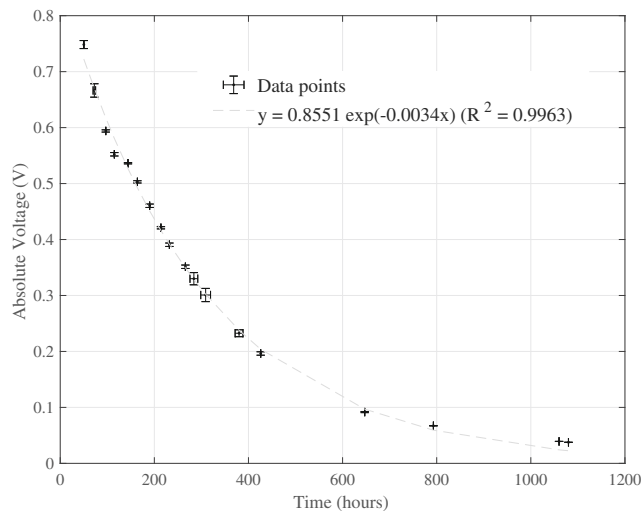
Fig. 5 Variation of output voltage of the monitoring system versus time after radioiodine administration. The error bars (k = 2) are shown which are less than 4%

agreement with [16], and the beta particle dose was dominant. This difference resulted in $CF_2 = 0.068$.

The absorbed dose rates in the right lobe from the first and the second simulations of section 2.3 were 0.67 and 0.68 mGy/s, respectively. Their difference resulted in $CF_1 = 0.017$. The absorbed dose rate in the phantom thyroid lobes and isthmus was determined by MC code as 0.68 mGy/s, while the MIRD calculation resulted in the dose rate of 0.72 mGy/s. Substitution of the obtained values in eq. (4) resulted in %DD = 1.0%. Agreement of the simulated and analytical dose calculations within 1% uncertainty permitted assignment of the achieved absorbed doses in each organ to the voltage reading from the IRD system. For example, the output voltage for system 1 after 50 h was 0.75 V (the first data point in Fig. 5). Taking the I-131 decay into account, it corresponded to $0.68e^{-0.0036 \times 50} = 0.57 \frac{mGy}{s}$. Therefore, the system was calibrated based on 0.76 mGy.s^{-1}.V^{-1} thyroid dose conversion coefficient. Because the minimum resolvable voltage was 0.038 V during the time-decay measurements, it can be deduced that minimum detectable activity by IRD system is 7.4 MBq (0.2 mCi) which corresponds to thyroid dose rate of 0.03 mGy/s. It is far below the routine activities encountered in clinic for safe release of the patient [17].

4 Discussion

A prototype version of an in vivo online thyroid monitoring dosimeter for use in radioiodine therapy was designed, developed, and evaluated technically. In order to find an optimum shape and size for system design, MC simulation was used. Then, two dosimeter modules suitable to be placed on the thyroid lobes were assembled and tested in vitro. The system was tested from linearity and long-term performance by I-131

isotope delivered to the phantom thyroid or the vial insert. In order to find a relationship between the delivered dose to thyroid and nearby normal organs to the voltage reading, MC simulation of the CT-scanned phantom was done. The simulation was validated analytically, and the calibration factor has been reported.

It was found that the system reading did not deviate from the linear performance for very high (8.2 GBq) and very low (7.4 MBq) activities encountered. It can be compared with the maximum linear performance range of CoTI device, 2000 cps, which is almost corresponding to 20 MBq [9]. The difference between the linear fit of the two systems (Fig. 4a) is due to difference in the radiation detector and photodiode covering, distance from the vial, and the quality of the coupling.

Figure 5 shows the voltage reading from one of the dosimeter modules versus time during 45 days of experiment. It shows similar decline as the physical decay constant of I-131 ($\lambda = 0.0036$ h^{-1} based on half-life = 8.05 d). The experiment on the phantom was performed merely to check the functionality of the system, especially the electronic module. Because there is no biologic decay during such an experiment, only the physical decay was detectable which is different with a real clinical situation. In addition, the long-term performance of the device from heating point of view was tested via this experiment. No disturbing heating was detected from the long-term performance.

Validation of the MC-based dose calculation was performed by application of two correction factors to compare to the MIRD-based dose calculation. Then, the IRD system reading was calibrated versus the calculated dose in the thyroids. Similarly, the reading can be calibrated versus absorbed dose in the nearby organs. For example, it was found that the spinal cord dose rate was 0.095 mGy/s with the initial activity using the MCNP simulation. Therefore, the spinal cord calibration factor was found equal to 0.10 mGy.s^{-1}.V^{-1} based on the methodology described in section 3.3. This approach can be extended to any other organ, and by providing the suitable calibration factors, the system is capable of reporting all desirable organ doses online.

5 Conclusion

A series of preliminary tests have been conducted on an iodine radionuclide dosimeter system. Based on this in vitro study, it is expected that it can be used to determine the absorbed doses in the target volume and organs at risk to manage the subsequent treatment steps during in vivo experiments. Also, it can be used for safe discharge of the patient from the hospital based on the recommendations. The system showed a linear response up to rarely used high activities and high sensitivity down to rarely used low activities. It did not show any deviation from the expected performance during the long-term use

which obviates a need for frequent recalibration. Based on a phantom simulation, the conversion coefficients for the thyroid and spinal cord doses were determined, and the approach can be extended to other organ dose determination. In summary, a light, linear, and handy monitoring system that can be constructed with reasonable price was developed ready to be upgraded for clinical evaluation.

Glossary of terms

Symbol	Name	Definition	Unit
ED	Energy deposition	Energy deposition per disintegration	keV/t
ED_{anal}	Analytical energy deposition	Calculated energy deposition per disintegration	keV/t
ED_{sim}	Simulated energy deposition	Monte Carlo-derived energy deposition per disintegration	keV/t
CF_1	The first correction factor	Factor accounting for backscattering from surrounding material and activity in nearby organs	–
CF_2	The second correction factor	Factor accounting for different applied energy spectra in analytical and simulation calculations	–
$EDsim'$	1st modified energy deposition	Temporary simulated energy deposition accounting for surrounding material and activity in nearby organs	keV/t
$EDsim''$	2nd modified energy deposition	Temporary simulated energy deposition accounting for different energy spectra	keV/t
$\%DD$	Percent dose difference	Difference between analytically calculated and corrected simulation doses	%

Compliance with ethical standards

Conflict of interest   The authors declare that they have no conflict of interest.

References

1. Lassmann M, Reiners C, Luster M (2010) Dosimetry and thyroid cancer: the individual dosage of radioiodine. Endocr Relat Cancer 17:R161–R172
2. Giostra A, Richetta E, Pasquino M, Miranti A, Cutaia C, Brusasco G, Pellerito RE, Stasi M (2016) Red marrow and blood dosimetry in 131 I treatment of metastatic thyroid carcinoma: pre-treatment versus in-therapy results. Phys Med Biol 61:4316–4326
3. Hanscheid H, Canzi C, Eschner W, Flux G, Luster M, Strigari L, Lassmann M (2013) EANM Dosimetry committee series on standard operational procedures for pre-therapeutic dosimetry II. Dosimetry prior to radioiodine therapy of benign thyroid diseases. European journal of nuclear medicine and molecular imaging 40: 1126–1134. https://doi.org/10.1007/s00259-013-2387-x
4. van Gils K, Brinks P, Lavalaye J, Verberne HJ, Habraken JBA (2017) A method to measure the absorbed dose of the thyroid during I-131 therapy, using a collar detector system and a SPECT acquisition. Med Phys 44:5450–5456. https://doi.org/10.1002/mp.12472
5. Sisson JC, Freitas J, McDougall IR, Dauer LT, Hurley JR, Brierley JD, Edinboro CH, Rosenthal D, Thomas MJ, Wexler JA, Asamoah E, Avram AM, Milas M, Greenlee C (2011) Radiation safety in the treatment of patients with thyroid diseases by radioiodine 131I: practice recommendations of the American Thyroid Association. Thyroid : official journal of the American Thyroid Association 21:335–346. https://doi.org/10.1089/thy.2010.0403
6. Venencia CD, Germanier AG, Bustos SR, Giovannini AA, Wyse EP (2002) Hospital discharge of patients with thyroid carcinoma treated with 131I. Journal of nuclear medicine : official publication, Society of Nuclear Medicine 43:61–65
7. Lee JH, Park SG (2010) Estimation of the release time from isolation for patients with differentiated thyroid Cancer treated with high-dose I-131. Nucl Med Mol Imaging 44:241–245. https://doi.org/10.1007/s13139-010-0041-0
8. Zuckier LS, Boardman B, Zhao QH (1998) Remotely pollable Geiger-Muller detector for continuous monitoring of iodine-131 therapy patients. Journal of nuclear medicine : official publication, Society of Nuclear Medicine 39:1558–1562
9. Brinks P, Van Gils K, Kranenborg E, Lavalaye J, Dickerscheid DBM, Habraken JBA (2017) Measuring the actual I-131 thyroid uptake curve with a collar detector system: a feasibility study. Eur J Nucl Med Mol Imaging 44:935–940. https://doi.org/10.1007/s00259-016-3595-y
10. Furstner M, Hentschel M, Spanjol PM, Prenosil GA, Weidner S, Krause T, Klaeser B (2017) Technical note: determination of individual thyroid clearance effective half-life with a common handheld electronic dosimeter. Med Phys 44:1558–1562. https://doi.org/10.1002/mp.12161
11. Knoll GF (2010) Radiation detection and measurement. 4th Ed. edn. John Wiley & Sons
12. Tavernier S (2010) Experimental Techniques in Nuclear and Particle Physics. 1st Ed. edn. Springer-Verlag Berlin Heidelberg
13. Pelowitz DB (2008) MCNPX USER'S MANUAL. Los Alamos National Laboratory, U.S.A
14. Ahmadi M, Ramezani M, Hariri-Tabrizi S, Azma Z (2019) Manufacturing and evaluation of a multi-purpose Iranian head and neck (MIHAN) anthropomorphic phantom. Phys med:(under review)
15. Amato E, Lizio D, Baldari S (2009) Absorbed fractions for photons in ellipsoidal volumes. Phys Med Biol 54:N479–N487. https://doi.org/10.1088/0031-9155/54/20/n02
16. Cember H, Johnson TE (2008) Introduction to health physics. 4th edn. McGraw-Hill Education
17. Mayles P, Nahum A, Rosenwald J (2007) Handbook of radiotherapy physics: theory and practice. Taylor & Francis Group, CRC Press, Boca Raton

Sanaz Hariri Tabrizi : She received the BS degree in biomedical engineering in 2005 and the MS and PhD degrees in medical radiation engineering in 2008 and 2013, respectively. She is now an assistant professor at Shahid Beheshti University.

Seyed Amir Hossein Feghhi : He completed his PhD and MS at Amirkabir University of Technology. Since 2009, he is a professor at the department of radiation applications, Shahid Beheshti University of Tehran. Since 2011, he is the vice chair for research.

Meysam Ramezani : He received his BS degree in biomedical engineering. This study was for fulfillment of his MS thesis in radiation applications at Shahid Beheshti University of Tehran. He is now working on development of the current system.

Parham Geramifar : He is an assistant professor at the school of medicine, Tehran University of Medical Sciences (TUMS). He received his PhD in medical radiation. His main research field is quantitative imaging, molecular imaging and Monte Carlo simulations.